Simplified Seismic Analysis of Disordered Masonry Towers

Simplified Seismic Analysis of Disordered Masonry Towers

Luca Facchini[1] and Michele Betti[2]

Abstract: The structural assessment of existing masonry towers under exceptional loads, such as earthquake loads, requires reliable and expedite methods of analysis. These approaches should take into account both the specific nonlinear behavior of the material (for instance, the small tensile strength) and the randomness that affect the masonry material's properties (in some cases the distribution of the elastic parameters too). Considering the need of simplified but effective methods to assess the seismic response of such a class of structures, the paper proposes an expeditious approach based on an equivalent Bouc and Wen model. As a prototype of masonry towers, a cantilever masonry beam is analyzed assuming that the first mode shape governs the dynamic behavior. With this hypothesis, the nonlinear Bouc and Wen model is employed to reproduce the system hysteretic response. Subsequently, assuming the material properties as random variables, stochastic linearization and the perturbative approach are employed to evaluate the bounds of the seismic response. The results of the simplified approach are compared with the results of finite-element models to show the effectiveness of the method. **DOI: 10.1061/AJRUA6.0000856.** *© 2015 American Society of Civil Engineers.*

Author keywords: Bouc and Wen model; Masonry towers; Nonlinear dynamics; Reliability assessment; Stochastic linearization; Perturbation methods; Disordered systems.

Introduction

The assessment of the structural response of masonry structures, especially in case of severe excitations such as the ones due to the seismic loading, must take into account the nonlinear mechanical behavior of the masonry components (small tensile strength and limited compressive strength). This nonlinear behavior is also characterized by a hereditary nature and, as a result, the restoring force that describes the mechanical behavior of the masonry structure cannot be simply described as a function of the instantaneous displacement or acceleration due to hysteresis phenomena (Casolo 1998; Betti et al. 2014). In addition, another element that needs to be taken into account to perform a reliable assessment of the structural response is the randomness that affects the masonry material's properties (in case of existing buildings, he spatial distribution of the elastic parameters as well).

Focusing on slender masonry structures, recent earthquakes showed, once again, the high vulnerability of such a typology of structure (Milani and Valente 2015; Decanini et al. 2012), highlighting the need of expeditious and effective methodologies of seismic risk assessment in order to allow proper retrofitting strategies. In this respect, in recent years, several simplified methods have been proposed to analyze the structural response of such mechanical systems. Betti et al. (2005) analyzed the response of slender masonry walls under turbulent wind, proposing an approach based on modal reduction. The material was assumed as nontensile resistant (NTR), while the mechanical properties as deterministic. Lucchesi and Pintucchi (2007) developed a one-dimensional deterministic numerical model to perform nonlinear dynamic analysis of slender masonry towers. The main mechanical characteristics of the material, in all the sections along the height, were taken into account by means of a nonlinear elastic constitutive law formulated in terms of generalized stress and strain. The material behavior was assumed NTR with limited compressive strength. To describe the dynamic response of slender masonry towers, a three-dimensional fiber model was proposed by Casolo (1998) and employed in deterministic vulnerability analysis: the structure consisted of a set of fibers aligned with the vertical axis of the tower, and the constitutive behavior of each single fiber was assumed hysteretic with damage. To account for the uncertainties deriving from the nonlinear behavior of masonry (and forcing actions), a statistical approach to estimate the combined effects of the most important factors governing the structural response (viscous damping, height, strength, stiffness, strain-softening, and hysteretic dissipating characteristics) was proposed and employed. An analysis method to account for material uncertainties to solve this class of mechanical problems was proposed by Facchini et al. (2005) where, based on a Galerkin approach, the material properties were assumed as a stochastic field. Other possible approaches to account for the randomness that affects the material properties are perturbation methods, originally proposed by Liu et al. (1986).

Despite many recent advances, the literature review still highlights the need of expeditious and effective approaches capable to effectively analyze the seismic response of slender masonry towers when the masonry is assumed as a random material. In this respect, recent studies show the high flexibility of the hysteretic model proposed by Bouc (1967), and subsequently improved by Wen (1976, 1980). The model has the advantage of its computational simplicity (since it requires only one auxiliary nonlinear differential equation to describe the hysteretic behavior) and, in addition, closed-form expressions are available that simplify the employment of the model in nonlinear random vibration problems. The Bouc and

[1]Associate Professor, Dept. of Civil and Environmental Engineering (DICeA), Univ. of Florence, via di Santa Marta 3, I-50139 Firenze, Italy. E-mail: luca.facchini@unifi.it

[2]Assistant Professor, Dept. of Civil and Environmental Engineering (DICeA), Univ. of Florence, via di Santa Marta 3, I-50139 Firenze, Italy (corresponding author). E-mail: mbetti@dicea.unifi.it

Note. This manuscript was submitted on February 26, 2015; approved on October 8, 2015; published online on December 22, 2015. Discussion period open until May 22, 2016; separate discussions must be submitted for individual papers. This paper is part of the ***ASCE-ASME Journal of Risk and Uncertainty in Engineering Systems, Part A: Civil Engineering***, © ASCE, ISSN 2376-7642.

Wen model has been extensively employed to describe a plethora of hysteretic behavior like degradation of stiffness and strength (Marano and Greco 2006; Erlicher et al. 2008), and Bouc and Wen (in the following, BW in short) models have been used in an wide range of applications such as vibration of steel structures (Oldfield et al. 2005), concrete structures (Wang et al. 2007; Bursi et al. 2012), wood joints (Foliente 1995), or base isolation devices for buildings (Ismail et al. 2010). The growing interest around this model is testified by the ever-increasing number of researches that employ such a model (Ismail et al. 2009).

The paper, analyzing the clarifying example of a disordered masonry cantilever beam, investigates the employability and the efficiency of the BW model in order to account for the nonlinear hysteretic phenomena that develop in slender masonry towers during seismic loading. To discuss the proposed approach, the paper is organized as follows: in the first part, two numerical models are introduced, developed with the finite-element (FE) technique. The numerical FE models were employed to perform nonlinear static and nonlinear dynamic analyses aimed to assess the behavior of a slender masonry tower under seismic loading. In the second part of the paper, the results of the numerical nonlinear analyses were employed as a reference to evaluate the parameters needed to tune the simplified Bouc and Wen model and to assess the effectiveness of the obtained results. In the third part, an equivalent linearization method and a perturbative approach were employed to account for the material randomness, where average values and bounds of the structural response were evaluated and discussed.

Nonlinear FE Reference Models

Two FE codes were employed to numerically evaluate and analyze the nonlinear response of a slender masonry beam under seismic load. The reference case study was a 10-m-wide (B), 40-m-high (H), and 1-m-thick cantilever masonry beam. The behavior of the masonry tower under seismic loads acting in the plane of the structure was analyzed by means of static nonlinear pushover analysis and dynamic nonlinear analysis. Results of the analyses were first compared with each other to assess their effectiveness, and subsequently employed to identify the parameters of the equivalent Bouc and Wen model.

Numerical Modeling with Code Aster

The first numerical model of the cantilever masonry beam was built by means of the open source software *Code_Aster*, a free finite-element code (distributed under the GNU GPL license) for the numerical simulation of materials and mechanical structures, developed by EDF (Électricité de France). The code was employed to build two numerical models: (1) a model built with 8-node three-dimensional (3D) elements having the dimensions of $0.5 \times 0.5 \times 0.5$ m, employed for the nonlinear static analyses; and (2) a model (with the same typology of finite elements, but having the dimensions of $1.0 \times 1.0 \times 1.0$ m) employed for the nonlinear dynamic analyses. The first model was characterized by 3,200 elements and about 15,120 degrees of freedom (DOFs), while the second one had 400 elements and about 2,640 DOFs.

In order to take into account the nonlinear behavior of the masonry, two types of mechanical damage models were considered. The nonlinear static analyses were performed with the damage model of Mazars (Mazars 1984; EDF R&D 2012), while for the nonlinear dynamic analyses, the Endo Orth Beton (Godard 2005; EDF R&D 2011) damage behavior was adopted. The first damage model is an isotropic scalar damage model, quite simple and robust (from a computational point of view), which has the limit of not taking into consideration the stiffness restoring due to the cracks closing. The second one is an anisotropic model that is able to take into account the cracks closing. Both mechanical models were originally introduced for the numerical modeling of concrete. Their effectiveness in order to reproduce the masonry non-linear behavior was evaluated by comparing the numerical results obtained with *Code Aster* with those obtained with the second FE code. The models need different parameters to identify the damage threshold but, in general, they require a reduced number of independent parameters to define the nonlinear behavior (Mazars 1984; Godard 2005). Both the Mazars and the Endo Orth Beton parameters were identified in order to fit the uniaxial compressive and tensile strength values reported in Table 1. Additional information about the identification of the model parameters can be found in Betti et al. (2012).

Table 1. Masonry Model Parameters

Parameter	Value
E_w (N/mm^2)	1,500
ν (-)	0.25
c (N/mm^2)	0.24
θ (°)	38
δ (°)	15
f_{wc} (N/mm^2)	5.00
f_{wt} (N/mm^2)	0.24

Note: c = cohesion; E_w = elastic modulus; f_{wc} = uniaxial compressive strength; f_{wt} = uniaxial tensile strength; v = poisson coefficient; θ = angle of internal friction; δ = dilatancy.

Numerical Modeling with ANSYS

As a second case, the masonry cantilever beam was modeled by means of the commercial FE code *ANSYS*. The model was built by means of 3D 8-node isoparametric finite-elements having the dimensions of $1.0 \times 1.0 \times 1.0$ m, and the final 3D model consisted of 400 *solid65* elements and about 2,640 DOFs.

To reproduce the nonlinear masonry behavior, the Drucker-Prager (DP) plasticity criterion (Drucker and Prager 1952), originally proposed for geomaterials, was employed. The material parameters required to define the model, the cohesion c, and the internal angle of friction φ, are usually introduced in such a way that the circular cone yield surface of the DP model corresponds to the outer vertex of the hexagonal Mohr-Coulomb yield surface (Fig. 1). The Drucker-Prager constitutive law can be written as follows:

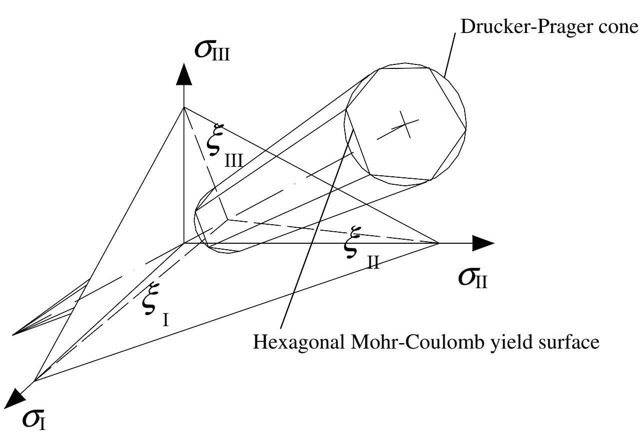

Fig. 1. Drucker-Prager yield surface in the Haigh-Westergaard stress space

ASCE-ASME J. Risk Uncertainty Eng. Syst., Part A: Civ. Eng., 2016, 2(2): C4015010

$$F = \alpha I_1 + \sqrt{J_2} - k = 0 \qquad (1)$$

where I_1 = first invariant of the Cauchy stress; J_2 = second invariant of the deviatoric part of the Cauchy stress; and α and k = two parameters required to define the yield DP surface. They are connected with the cohesion c and the friction angle φ by the following equations:

$$\alpha = \frac{2\sin\varphi}{\sqrt{3}(3-\sin\varphi)}; \qquad k = \frac{6c\cos\varphi}{\sqrt{3}(3-\sin\varphi)} \qquad (2)$$

The cohesion c and the angle of internal friction φ are thus the only two material parameters needed to define the yield surface. In this application, the DP criterion was combined with the Willam and Warnke (WW) failure criterion, originally proposed for concrete (Willam and Warnke 1975), which accounts for both cracking and crushing failure modes through a smeared model. With these assumptions, the masonry was modeled as an isotropic continuum capable to exhibit plastic deformation, to crack owing to traction and to crush owing to compression. Both the DP and WW criteria have been frequently employed to model the mechanical behavior of (complex) masonry structures. The WW criteria was used by Adam et al. (2009) to model the cracking and crushing capabilities of materials, and the comparison between numerical and experimental results show a good agreement. Among others, Betti and Vignoli (2008) combined the DP criterion with the WW failure surface to discuss, through a macroelement approach, the seismic vulnerability of an historic masonry church.

The assignment of the mechanical parameters required by the DP and WW criteria requires a careful calibration and, in the present study, being the analyses mainly aimed to assess the effectiveness of an equivalent BW hysteretic system, these parameters were assumed on the basis of available literature results for a stone masonry wall (Chiostrini et al. 1998). The adopted values are reported in Table 1 for both the linear (Young's modulus E and Poisson coefficient ν) and the nonlinear parameters of the masonry materials. The *ANSYS* model was employed to perform both static pushover and dynamic nonlinear analyses. The nonlinear system of equations was solved by an incremental Newton-Raphson method with arc-length control.

Code Aster—ANSYS Comparison

As a first comparison between the two FE codes, a static nonlinear pushover analysis was performed assuming a uniform distribution of horizontal loads along the height of the cantilever beam. The results were consequently compared analyzing both the damage (*Code Aster*) versus cracking/crushing (*ANSYS*) patterns and the corresponding capacity curves. Fig. 2 compares the capacity curves (resultant load versus displacement). Despite the different mechanical laws adopted to account for the nonlinear modeling of masonry, both codes offered a reliable estimation of the collapse load. A minor difference is instead observable in the maximum displacement (the horizontal displacement of the center of mass of the beam's top section is about 550 mm with the *Code Aster* model and about 320 mm with the *ANSYS* model). This is due to the fact that the nonlinear system of equations in *Code Aster* were solved by a displacement control method while a force control (Newton-Raphson) approach was employed with *ANSYS*.

A second comparison was made by means of nonlinear time-history analyses. As base input, the natural acceleration record of Colfiorito NS (North–South) 1997, scaled at PGA (peak ground acceleration) = 0.1 g, was employed (Fig. 3). Fig. 4 compares the time-histories of the base shear obtained with both codes, at increasing PGA of the scaled Colfiorito record (PGA = $0.20g$ and PGA = $0.26g$). Fig. 5 reports, for both codes, the numerical

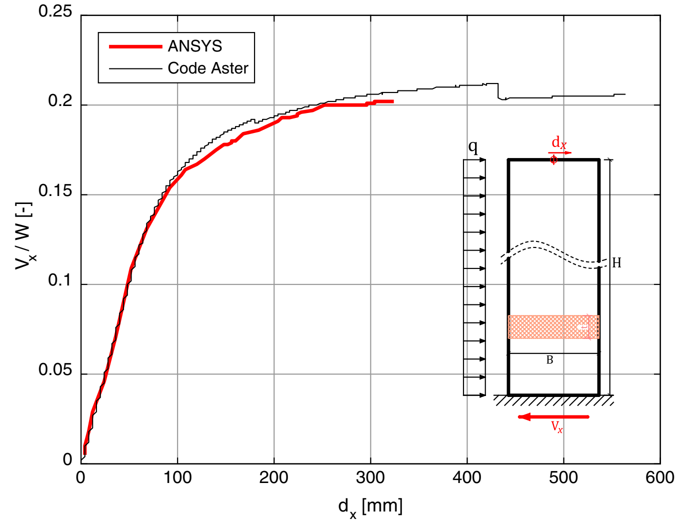

Fig. 2. Load-displacement curve *Code Aster* (Mazars model) and *ANSYS* comparison ($B = 10$ m, $H = 40$ m)

time-histories of the displacement of the center of mass of the top section (again at increasing PGA). It is still possible to observe that, despite few differences (between 8 and 12 s), both codes offered consistent results.

Additional assessments of the employed numerical models are reported in a paper recently published by Bartoli et al. (2013). The authors, investigating the collapse behavior of masonry structures, analyzed the consistency of the results (collapse load, collapse displacement, and the load-displacement equilibrium path) obtained using 10 different numerical approaches, including the models herein adopted. The comparison of the results confirms the robustness and the effectiveness of the employed models.

Approximation of the Tower Response with the Bouc and Wen Model

The cantilever masonry beam was analyzed assuming that the first mode shape governs the whole dynamic behavior. Based on this hypothesis, the ability of the nonlinear hysteretic Bouc and Wen

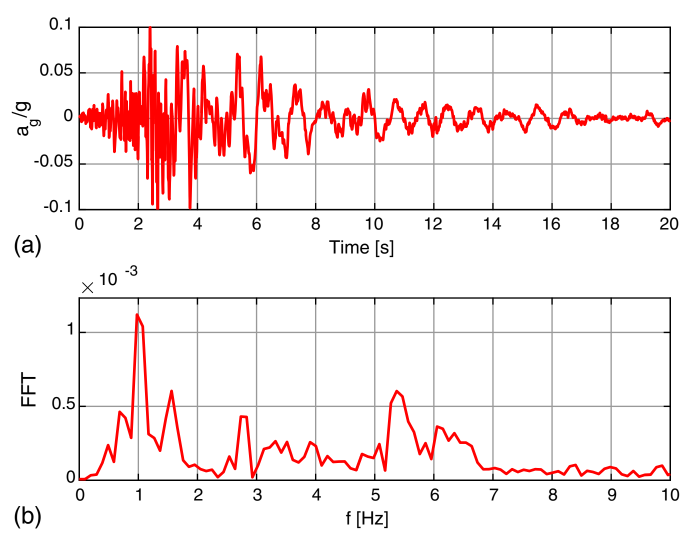

Fig. 3. Colfiorito NS 1997 acceleration: (a) time history; (b) FFT

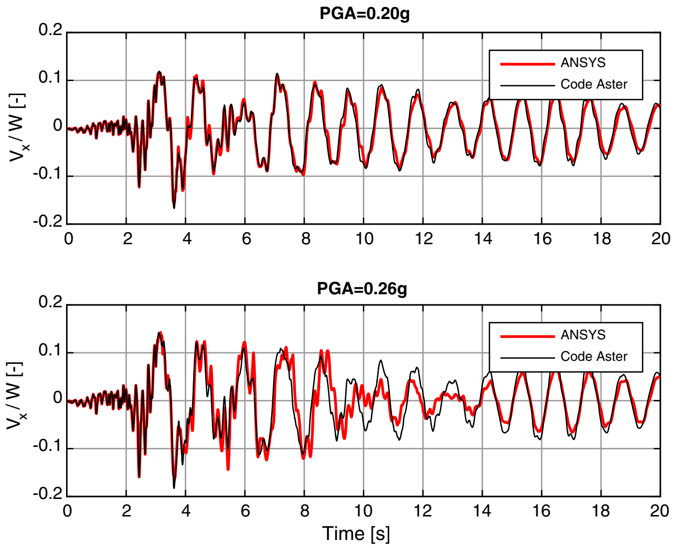

Fig. 4. Base shear time history at different PGA

model to reproduce the system response was investigated and the results of the proposed approach were compared with the results of the finite-element (FE) models to discuss the effectiveness of the approximation.

When a BW model is employed in practical applications, the first step is to identify (tune) the model parameters. By appropriately choosing a set of parameters, it is possible to reproduce the actual hysteresis loop of a plethora of mechanical systems. Given a set of experimental or numerical input/output data, the model parameters must be tuned so that the output of the BW model matches as well as possible the reference data. Once the BW model parameters have been identified, the resulting model can be considered as a good approximation of the original investigated hysteretic system. Herein, the BW model parameters were identified by comparing the behavior of the BW model with the response of the masonry cantilever beam subjected to a static horizontal load (evaluated through the FE analysis developed in the previous section). The horizontal displacement of the center of mass of the

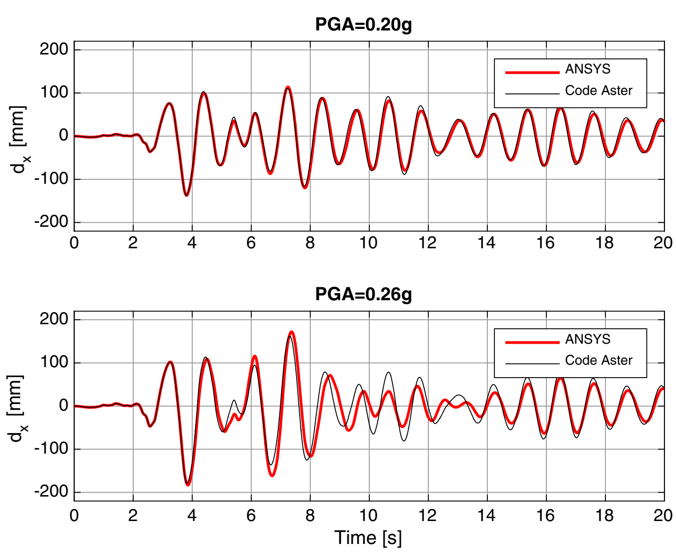

Fig. 5. Displacement time history (center of mass of the upper section of the masonry beam) at different PGA

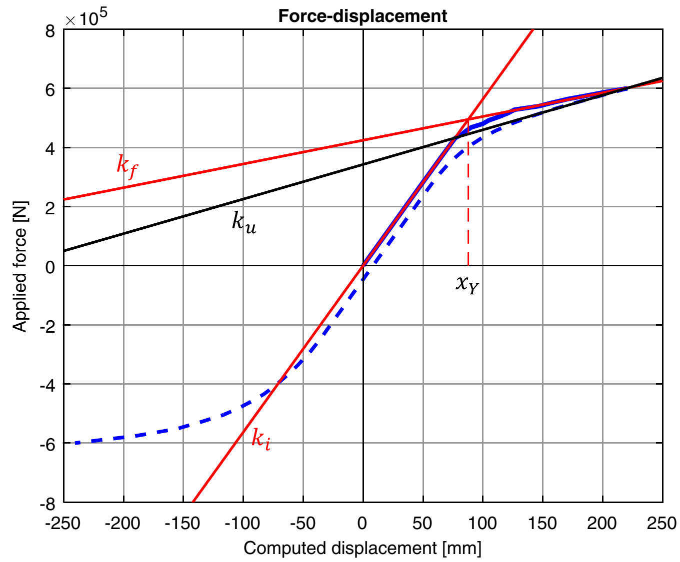

Fig. 6. Applied force–computed displacement curve (*ANSYS* analysis under cyclic loading)

cantilever beam's top section, shown in Fig. 6 (the applied force—computed displacement curve is obtained with the *ANSYS* FE model) exhibits slight but clearly-visible hysteretic behavior.

Single Degree-of-Freedom Model Assumption

From the results of the structural analyses performed by means of *Code Aster* and *ANSYS*, it can be inferred that the dynamic behavior of the cantilever beam can be accurately modeled by means of its first mode shape. The first three mode shapes (obtained with the *ANSYS* code) are reported in Fig. 7; the first one activates about the 76% of the total mass. Therefore, an equivalent nonlinear single degree-of-freedom (SDOF) system can be defined, whose degrading stiffness can be determined by means of the performed nonlinear numerical analyses. Taking into account that *Code Aster* and *ANSYS* give the same results, the ones obtained with *ANSYS* were considered as reference. Fig. 6 reports the results (load versus displacement) of the static nonlinear analyses performed with *ANSYS* by applying a monotonically increasing/decreasing horizontal displacement at the top section of the masonry beam, in such a way to obtain the first-loading curve and the subsequent unloading curve. This result was taken into consideration to approximate the system behavior with the BW model, as reported next.

Identification of the Bouc and Wen Model Parameters

The behavior of the equivalent BW oscillator can be described by an incremental equation of motion of the form

$$m\ddot{x}(t) + c\dot{x}(t) + kg(t) = f(t) \tag{3}$$

where m = mass of the system; c = viscous linear damping coefficient; $x(t)$ = displacement; $kg(t)$ = nonlinear restoring force (k denotes the stiffness of the system); and $f(t)$ = external excitation. The overdots in the $x(t)$ variables represent the derivative with respect to time.

According to the BW model, the restoring force function was assumed as a linear combination of a linearly-elastic force and a history-dependent term

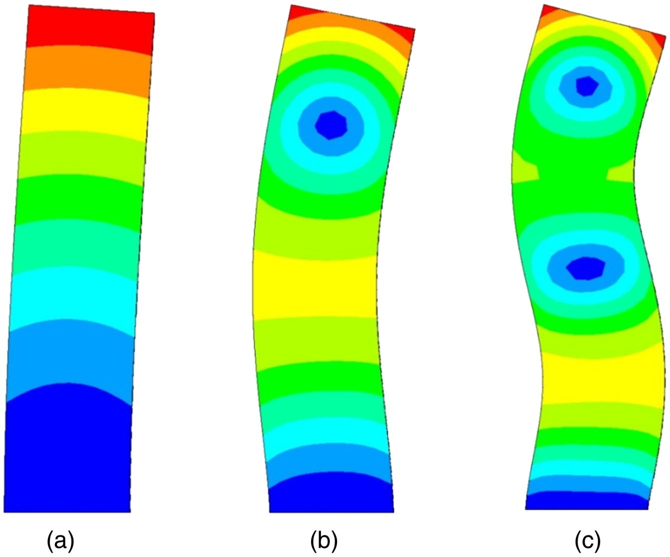

Fig. 7. First three mode shapes of the cantilever masonry beam: (a) first mode ($f_1 = 0.88$ Hz); (b) second mode ($f_2 = 4.59$ Hz); (c) third mode ($f_3 = 10.73$ Hz)

$$kg(t) = k\alpha x(t) + k(1-\alpha)z(t) \tag{4}$$

In Eq. (4) $k\alpha x(t)$ = elastic component (instantaneous response) while $k(1-\alpha)z(t)$ = hysteretic component (which depends on the past history of stresses and strains); α = relation between the final and the initial stiffness ($0 < \alpha < 1$); and $z(t)$ = so-called hysteretic displacement (a fictitious displacement). This hysteretic displacement is given by the following differential equation (with initial condition $z(0) = 0$):

$$\dot{z}(t) = \dot{x}(t)\{A - \mid z \mid^n \cdot [\beta + \gamma \mathrm{sgn}(\dot{x})\mathrm{sgn}(z)]\} \tag{5}$$

where $\mathrm{sgn}(\cdot)$ = *signum* function.

The differential Eqs. (3)–(5) contain five nondimensional unspecified parameters that can be chosen to generate a broad range of different hysteresis loops. According to this representation, the first set of parameters, which controls the shape and the size, of the hysteresis loop to be identified, is composed by $\{A, k, \alpha, n, \beta$, and $\gamma\}$. Several studies have been conducted to quantify the importance of each parameter on the overall response of different hysteretic structures in the BW model, and to classify the parameters accordingly. The manner in which the parameters of the BW model influence the shape of the hysteresis loop was recently analyzed by Ikhouane et al. (2007). In their research, the authors study in depth the relationship between the parameters that appear in the differential equation and the shape of the obtained hysteresis loop.

To identify the nondimensional parameters, several methods have been proposed in literature based on simulated or experimental input/output data. According to Ismail et al. (2009) and Ortiz et al. (2013), the procedures employed in literature to identify the parameters of the BW models can be classified into two major families: (1) methods based on the minimization of a loss function, and (2) methods based on nonlinear filtering. In this paper, the identification of the BW model used a method included in the first category, and based on a mixed two-step procedure. The method combines results coming from both static and time-history numerical analyses, with the BW parameters optimized so that $x(t)$ may approximate the displacement of the center of mass of the cantilever tower's top section. In particular, results obtained by means of the pushover analysis were employed to identify the six parameters $\{A, k, \alpha, n, \beta$, and $\gamma\}$. The remaining ones (mass m and viscous linear damping coefficient c of the equivalent BW system) were obtained by means of the calibration of the dynamic response of the BW model with respect to the dynamic simulated response of the FE model.

Among the six parameters that must be identified, it was shown (Cunha 1994; Facchini et al. 2012) that parameter A in Eq. (5) can be considered redundant, and hence next it was considered as unitary ($A = 1$) without loss of generality.

The second parameter, k, the stiffness of the equivalent oscillator, can be obtained by finding the derivative of the nonlinear restoring function $kg(t)$ with respect to the displacement x, obtaining the following expression for the tangent stiffness k_t:

$$\begin{aligned} k_t &= k\frac{\partial g}{\partial x} = k\left[\alpha + (1-\alpha)\frac{\partial z}{\partial x}\right] = k\left[\alpha + (1-\alpha)\frac{\dot{z}}{\dot{x}}\right] \\ &= k\{\alpha + (1-\alpha)[A - (\beta + \gamma\mathrm{sgn}(\dot{x})\mathrm{sgn}(z)) \mid z \mid^n]\} \end{aligned} \tag{6}$$

Having assumed the parameter A as unitary, and considering the initial conditions $z(0) = 0$, parameter k_t reduced to the initial stiffness k_i of the system, and the initial stiffness can be computed through Eq. (6) obtaining:

$$\{z(0) = 0; A = 1\} \Rightarrow k_i = k_t|_{z=0} = k[\alpha + (1-\alpha)] = k \tag{7}$$

The postelastic stiffness, k_f, according to Marano and Greco (2006), is given as $k_f = \alpha k$; hence the following relation holds asymptotically:

$$\dot{z} = 0 \Rightarrow k_t = k_f = \alpha k \Rightarrow \alpha = \frac{k_f}{k_i} \tag{8}$$

When the maximum displacement is reached and the unloading process begins, the following expression holds for the unloading initial stiffness k_u:

$$\left.\begin{array}{r} z = \hat{z} = 1/(\gamma+\beta)^{1/n} \\ \mathrm{sgn}(z) = 1; \mathrm{sgn}(\dot{x}) = -1 \end{array}\right\} \Rightarrow k_u = k\left\{\alpha + (1-\alpha)\left[1 - \frac{\beta-\gamma}{\beta+\gamma}\right]\right\} \tag{9}$$

and

$$\frac{\beta-\gamma}{\beta+\gamma} = \frac{1-(k_u/k)}{1-\alpha} = \frac{k_i - k_u}{k_i - k_f} \tag{10}$$

Finally, the elastic limit displacement can be expressed, according to Cunha (1994), as

$$\beta + \gamma = x_Y^{-n} \tag{11}$$

Therefore, only one parameter, n, or alternatively β or γ, remained undetermined: the parameter n influences the transition from elastic to postelastic behavior and the distance of the unloading path from the first loading, while the ratio β/γ affects the transition from the loading to the unloading curve (Ikhouane et al. 2007).

The numerical analyses enable direct estimation a few of the BW parameters: the initial stiffness $k_i = 5{,}654$ N/mm, the ratio $\alpha = k_f/k_i = 0.1395$, and the limit elastic displacement $x_Y =$ 90 mm (Table 2). These values were assumed as fixed, and consequently the remaining parameters to be identified were $\{n$, or β, and $\gamma\}$.

As a first attempt, the value of the exponent n was assumed equal to 5. With this assumption, the hysteresis loop shown with

Table 2. BW Model Parameters Identification

Parameter	First	Second
k_i (N/mm)	5,654	5,654
k_f (N/mm)	789	789
k_u (N/mm)	1,171	793
x_Y (mm)	90	90
n (-)	5.0	4.0
α (-)	0.1395	0.1395
β (-)	1.627×10^{-10}	1.523×10^{-8}
γ (-)	6.656×10^{-12}	6.646×10^{-12}

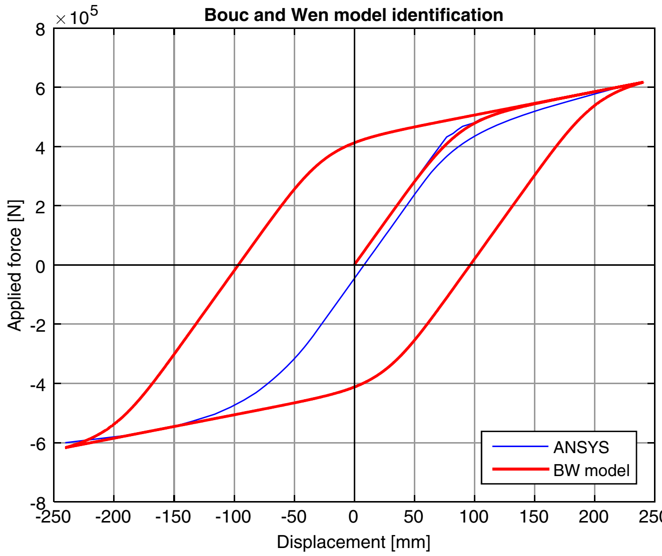

Fig. 8. Comparison of the identified BW model with the *ANSYS* results (first attempt)

a thick line in Fig. 8 was obtained. It is possible to observe that $n = 5$ reproduced correctly the transition from the elastic to the postelastic branch, but the overall behavior of the oscillator was very poor. As a second attempt, n and the unloading initial stiffness k_u were both lowered (Table 2), obtaining the behavior reported in Fig. 9. This choice gave better results, with an energy dissipation cycle very close to the reference one (obtained with the FE code).

Once the restoring function $g(t)$ was modeled (i.e., the parameters $\{k, \alpha, A, n, \beta,$ and $\gamma\}$ were identified), the two subsequent parameters that needed to be evaluated were the mass m and the damping c of the equivalent systems reported in Eq. (3). A hint can be drawn from the FE model. Assuming the participating mass associated with the first mode shape, the dynamic response of the identified BW oscillator was compared with the dynamic response of the cantilever beam (evaluated with *ANSYS*), and the comparison is shown in Fig. 10. The nonlinear dynamic analyses were performed employing the El Centro NS 1940 earthquake. It is possible to observe that the equivalent SDOF BW oscillator agrees quite well with the more complex, and computational demanding FE model elaborated with *ANSYS* (Fig. 10); however, the worst error committed on the response peaks was about 20%.

To overcome this error, a possibility is to identify mass and damping of the equivalent BW system by means of the analysis of the overall seismic response of the cantilever beam. To perform this optimization, the following error function (to be minimized over the whole time history) was considered:

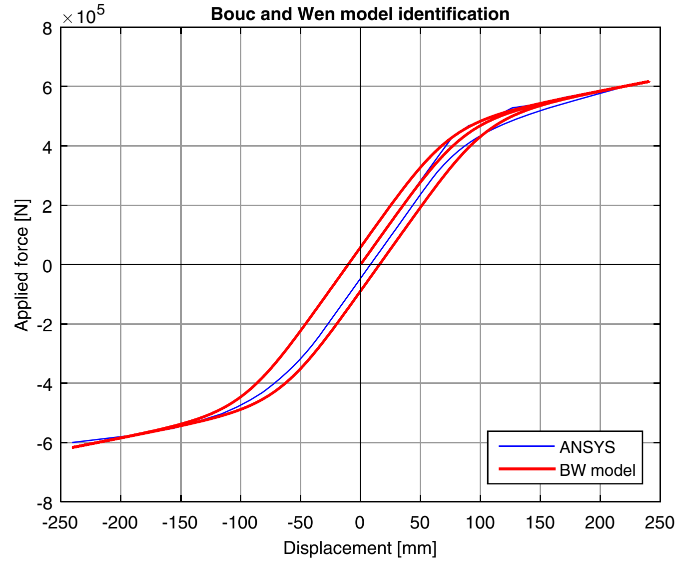

Fig. 9. Comparison of the identified BW model with the *ANSYS* results (second attempt)

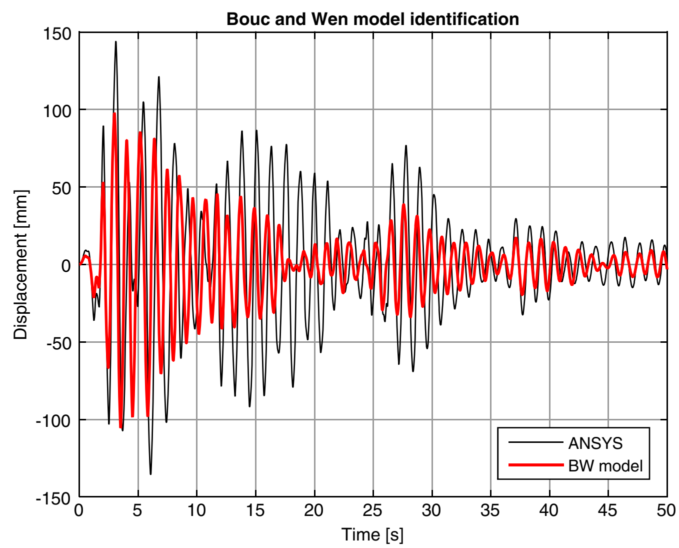

Fig. 10. Displacement time history: comparison between BW identified model and *ANSYS* results (second attempt)

$$\varepsilon = \int_0^T \frac{|w(x_{\rm ref}) \cdot (x_{BW} - x_{\rm ref})|}{|w(x_{\rm ref}) \cdot x_{\rm ref}|} dt \tag{12}$$

where x_{BW} = BW model displacement response; $x_{\rm ref}$ = FE model response; and w = weight function defined as follows:

$$w(x_{\rm ref}) = \frac{\exp[K_w|x_{\rm ref}|/(|x_{\rm ref}|)_{\max}]}{\exp(K_w)} \tag{13}$$

The weight function $w(x_{\rm ref})$ decreases exponentially for decreasing values of $|x_{\rm ref}|$. In particular, if the reference response $x_{\rm ref} \to 0$, then $w(x_{\rm ref}) \to \exp(-K_w)$; on the other hand, when the response $|x_{\rm ref}| \to (|x_{\rm ref}|)_{\max}$, then the weighting function tends to 1 and therefore the errors on the peaks of the response are much more important than the errors committed when the displacement of the system is small. The parameter K_w calibrates the importance

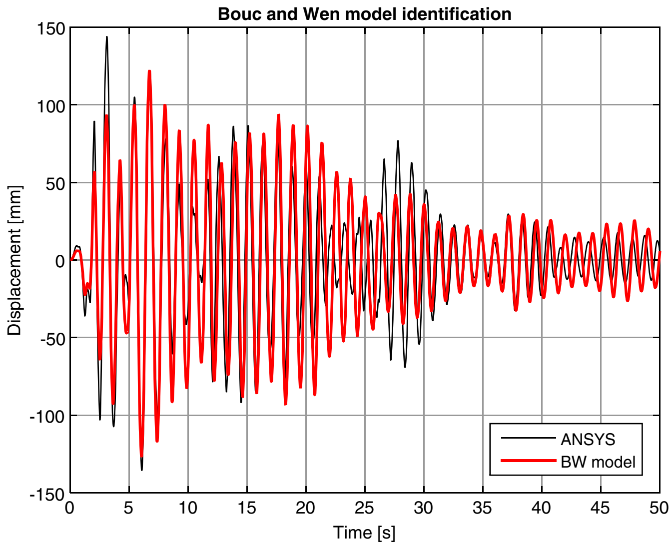

Fig. 11. Displacement time history: comparison between BW identified model and *ANSYS* results (optimization of mass and damping of the BW SDOF system)

of the errors committed near the response peaks (with respect to the other configurations of the system). If $K_w = 0$ then the weight function is 1 for any value of $|x_{\mathrm{ref}}|$, while for increasing values of K_w the errors near the peaks of the reference response become more and more significant. Herein, $K_w = 5$ was assumed.

According to this approach, the optimized system mass m and damping c were obtained, and results of this optimization, illustrated in Fig. 11, show a good agreement between the simulated FE results and the identified BW oscillator.

Disordered BW Oscillator

After calibration of the parameters $\{k, \alpha, A, n, \beta, \gamma, m, \text{and } c\}$ of the equivalent BW oscillator, the hysteretic model was employed to analyze the behavior of the disordered oscillator to evaluate the influence of the random stiffness on the tower response. The problem may have relevant impact on seismic assessment since masonry mechanical parameters, such as Young's modulus, are often difficult to estimate, especially for historic buildings. Possibilities can be in situ tests (by means of flat jacks) and even laboratory tests on small samples of the examined masonry, but the results can only give a local estimate of the parameters, which are necessarily affected by a more or less pronounced randomness.

To analyze the disordered system, two approaches were herein assumed. A first one considered a stochastic equivalent linearization of the equivalent BW model; the second one employed a perturbation approach directly on the equation of motion. The two approaches are next introduced and discussed.

Equivalent Disordered Linear System

The stochastic equivalent linearization method is considered to be one of the most powerful (approximate) techniques to analyze the nonlinear random response of mechanical systems (Wen 1980; Faravelli et al. 1988; Cunha 1994). To build the stochastic equivalent system, an energetic criterion was herein employed. Imposing a harmonic loading to the system, the energy dissipation due to the hysteretic cycles was negligible until the amplitude of the displacement reached a limit value x_M; above this threshold, the dissipated energy depended linearly on the amplitude of the actual displacement and was approximated by means of the following relation:

$$E_d \approx \max\{0, K_d \cdot (X - x_M)\}\,\mathrm{N\,mm} \tag{14}$$

where $X > 0$ = actual displacement amplitude (and K_d is a coefficient depending on the system properties). The energy dissipated by the equivalent system can be written as follows:

$$E_{d,e} = \oint c_e \dot{x} dx \tag{15}$$

By equating Eqs. (14) and (15), it was possible to estimate the equivalent damping c_e. The equivalent stiffness k_e was evaluated by computing the actual secant stiffness. The probabilistic structure of the response of the equivalent linear system was consequently evaluated numerically through an iterative procedure by using the standard techniques for linear systems. The iteration loop consisted in solving the equation of motion of the equivalent linear system from given values of the equivalent damping c_e and the equivalent stiffness k_e, and then, iteratively, computing updated values for c_e and k_e.

After setting up the equivalent linear system, the dependence of the equivalent stiffness and damping coefficients on the parameters of the BW model was first analyzed, and the disordered equivalent linear system was next computed. The Young's modulus of the masonry was considered a normally distributed random parameter with c.o.v. (coefficient of variation) = 0.1; this leads to a randomness of the initial stiffness, which can be considered normally distributed as well, with mean $\mu_{k_i} = 5{,}654$ N/mm and c.o.v. = 0.1. The final (postyielding) stiffness was assumed to be strictly dependent on the initial stiffness: $k_f = \alpha k_i$.

The forcing process taken into consideration in the simulations was the NS component of the 1940 El Centro earthquake, which can be modeled as a time-modulated stationary acceleration with the following parameters:

$$a_g(t) = \chi(t) a_{gs}(t) \quad \chi(t) = \frac{e^{-at} - e^{-bt}}{e^{-at_0} - e^{-bt_0}}$$
$$t_0 = \frac{\log(a) - \log(b)}{a - b} \quad S_{aa}(\omega) = S_0 \frac{\omega_0^4 + 4\xi_0^2\omega_0^2\omega^2}{(\omega^2 - \omega_0^2)^2 + 4\xi_0^2\omega_0^2\omega^2} \tag{16}$$

where $\chi(t)$ = time envelope; and $a_{gs}(t)$ = stationary part of the ground acceleration, defined by the Kanai-Tajimi PSDF (Power Spectral Density function) $S_{aa}(\omega)$ with parameters $\omega_0 = 12.5\,\mathrm{rad/s}$, damping $\xi_0 = 0.60$, and intensity $S_0 = 5.3 \cdot 10^5\ \mathrm{mm^2/s^3}$. The parameters a and b calibrate the shape of the time envelope of the accelerogram (they influence the build-up of the seismic action as the instant of maximum intensity is given by t_0, as well as the decay of the ground acceleration). The obtained values are: $a = 0.058\ \mathrm{s}^{-1}$; $b = 2.511\ \mathrm{s}^{-1}$; and $t_0 = 1.533$ s.

Introducing the variation on the initial stiffness k_i of the BW model, and accordingly on the final stiffness k_f, the stiffness k_e of the equivalent linear system was found to vary linearly and the damping hyperbolically. The empirical relations found were (Fig. 12)

$$k_e \approx (0.411 k_i - 73)\ \mathrm{N/mm} \qquad \xi_e \approx \frac{4270}{k_i^{1.2879091}} \tag{17}$$

In this way, the equivalent linear system with random stiffness and damping can be studied, subjected to the El Centro NS 1940 acceleration:

ASCE-ASME J. Risk Uncertainty Eng. Syst., Part A: Civ. Eng., 2016, 2(2): C4015010

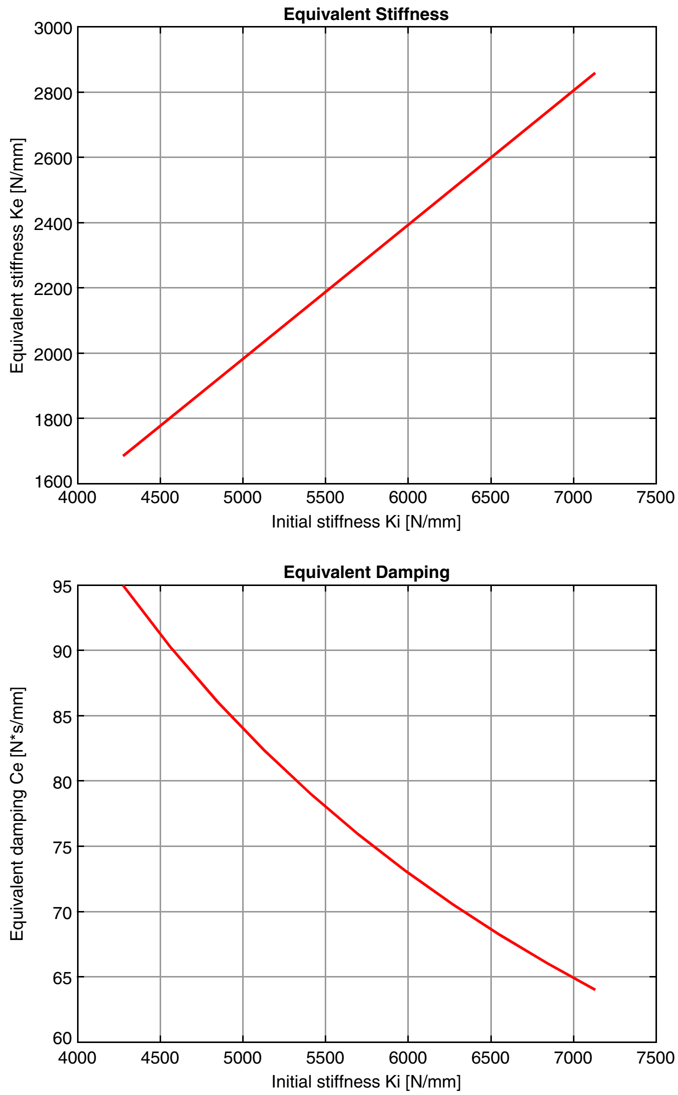

Fig. 12. Variation of the stiffness and the damping coefficient of the equivalent linear system caused by a variation in the initial stiffness of the BW model (final stiffness of the BW model is varied accordingly)

$$\ddot{x}_e + 2\xi_e \omega_e \dot{x}_e + \omega_e^2 x_e = -\chi(t) a_{gs}(t) \tag{18}$$

To solve the problem, a further approximation was introduced. The envelope of the ground acceleration was assumed to vary slowly with respect to acceleration itself. Under this assumption and taking into account the values obtained for the equivalent stiffness, the equivalent response x_e can be modeled as well as a stationary noise modulated by an envelope which, after some calculations, turns out to be the same as $\chi(t)$; therefore

$$x_e(t) = \chi(t) x_{es}(t) \Rightarrow \ddot{x}_{es} + 2\xi_e \omega_e \dot{x}_{es} + \omega_e^2 x_{es} = -a_{gs}(t) \tag{19}$$

Following a perturbation approach (Liu et al. 1986), the mean of the response vanishes, while the variance can be approximated by the following first-order expansion:

$$\sigma_{x_e}^2 \cong \left(\frac{\partial \bar{x}_e}{\partial k_i}\right)^2 \sigma_{k_i}^2 \qquad \ddot{\bar{x}}_e + 2\bar{\xi}_e \bar{\omega}_e \dot{\bar{x}}_e + \bar{\omega}_e^2 \bar{x}_e = -a_g(t)$$
$$\ddot{\bar{x}}_{e,k_i} + 2\bar{\xi}_e \bar{\omega}_e \dot{\bar{x}}_{e,k_i} + \bar{\omega}_e^2 \bar{x}_{e,k_i} = -(\bar{\xi}_{e,k_i} \bar{\omega}_e + \bar{\xi}_e \bar{\omega}_{e,k_i}) \dot{\bar{x}}_e - (\omega_e^2)_{,k_i} \bar{x}_e \tag{20}$$

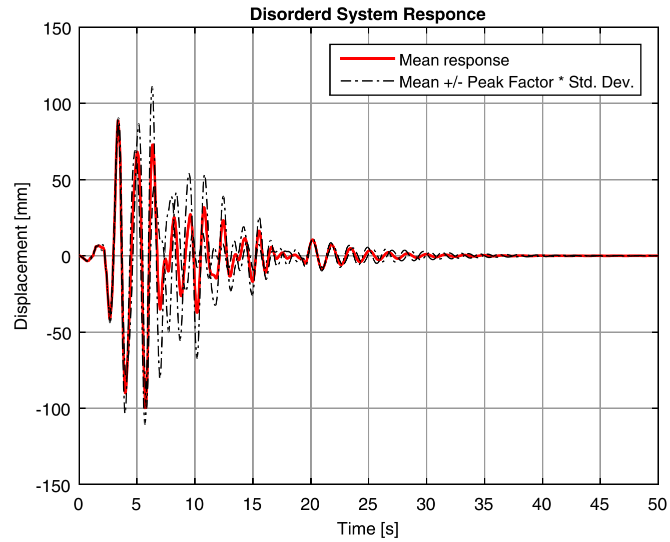

Fig. 13. Computed σ-bounds of the response of the disordered equivalent linear system to El Centro 1940 earthquake (North–South component)

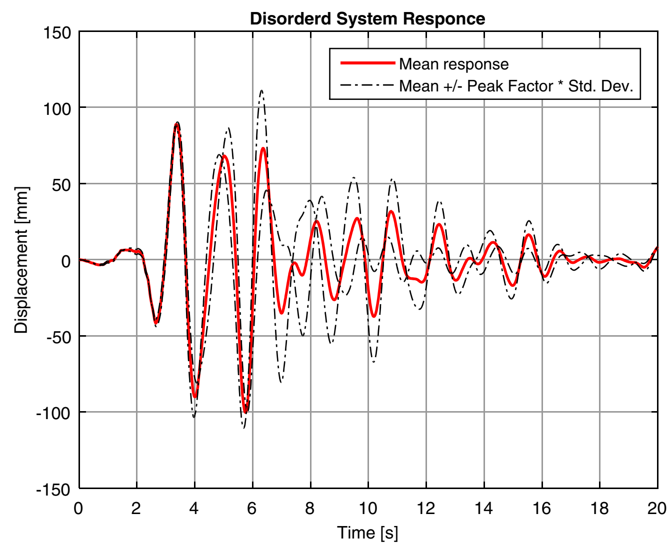

Fig. 14. Computed σ-bounds of the response of the disordered equivalent linear system to Colfiorito 1997 earthquake (North–South component)

where the overbar denotes the quantity evaluated for the mean value of k_i.

The integration of the perturbed equations (20) leads to the evaluation of the peak response of the equivalent linear system as the sum of the mean response, plus a peak factor times the standard deviation of the response itself. The peak factor, a simplified expression of the expected value of the envelope of a stationary narrow-band Gaussian process (Crandall and Mark 1963), was assumed as $g = \sqrt{(\pi/2)}$. Fig. 13 reports the computed bounds of the response of the disordered equivalent linear system subjected to the El Centro NS 1940 earthquake; while Fig. 14 reports the results obtained assuming the Colfiorito NS 1997 earthquake.

An attracting feature of the equivalent linearization approach is that it allows, in a straightforward manner, to obtain the inelastic response spectrum (IDRS) of the examined structure through the direct combination of the equivalent linear system parameters with the linear response spectrum of a given site (Roberts and Spanos 2003; Giaralis and Spanos 2013). This can lead to the definition of the seismic vulnerability of a group of towers that lie in a seismically homogeneous area.

Direct Perturbative Approach

As a second method, a perturbative approach, was directly employed and, also in this case, a randomness of the material stiffness was considered (a normal distribution with c.o.v. = 0.1). Based on this perturbative approach [Liu et al. (1986), and successively improved by Chiostrini and Facchini (1999)] the system response $x(t)$ and the history-dependent term $z(t)$ were directly approximated by means of a series expansion on the random parameter k

$$\begin{aligned} x(t,k) &\simeq \bar{x} + (k-\bar{k})\bar{x}_k + 1/2(k-\bar{k})^2\bar{x}_{kk} \\ z(t,k) &\simeq \bar{z} + (k-\bar{k})\bar{z}_k + 1/2(k-\bar{k})^2\bar{z}_{kk} \end{aligned} \tag{21}$$

The terms $\bar{x}_k$ and $\bar{z}_k$ representhe so-called sensitivity vectors (Liu et al. 1986) and must be computed with their derivatives. The solving equations are the derivatives of the equation of motion with respect to the random parameter k

$$\begin{aligned} &m\ddot{\bar{x}}(t) + c\dot{\bar{x}}(t) + kg_0(t) = f(t) \\ &g_0(t) = \alpha\bar{x}(t) + (1-\alpha)\bar{z}(t) \\ &\dot{\bar{z}}(t) = \dot{\bar{x}}(t)\{1 - |\bar{z}|^n \cdot [\beta + \gamma\mathrm{sgn}(\dot{\bar{x}})\mathrm{sgn}(\bar{z})]\} \end{aligned} \tag{22}$$

and

$$\begin{aligned} m\ddot{\bar{x}}_k(t) + c\dot{\bar{x}}_k(t) + kg_1(t) &= -g_0(t) \\ g_1(t) &= \alpha\bar{x}_k(t) + (1-\alpha)\bar{z}_k(t) \\ \dot{\bar{z}}_k(t) = \dot{\bar{x}}_k(t)\{1 - |\bar{z}|^n &\cdot [\beta + \gamma\mathrm{sgn}(\dot{\bar{x}})\mathrm{sgn}(\bar{z})]\} \\ &+ \dot{x}(t)(1 - n|\bar{z}|^{n-1}\mathrm{sgn}(\bar{z})\bar{z}_k \cdot [\beta + \gamma\mathrm{sgn}(\dot{\bar{x}})\mathrm{sgn}(\bar{z})] \\ &- |\bar{z}|^n \cdot \{\beta + \gamma D_k[\mathrm{sgn}(\dot{\bar{x}})\mathrm{sgn}(\bar{z})]\}) \end{aligned} \tag{23}$$

In Eqs. (21)–(23), the overbar indicates that the corresponding variable was evaluated in correspondence of the mean value of the uncertain structural parameters (stiffness k). The overdot indicates differentiation with respect to time; x_k, z_k, x_{kk}, and z_{kk} indicate the first and second derivatives of x and z with rpect to stiffnes k. The computation of the sensitivity vectors requires the solving of Eqs. (22)–(23), where a derivative (D_k) of the *signum* function appears: it implies differentiation with respect to k of a product of two *signum* functions, which involves considerable numerical difficulties.

To overcome this problem, the *signum* function was approximated with

$$s(x) = \frac{2}{\pi}\tan^{-1}(cx) \tag{24}$$

where the parameter c was assumed as $c = 5.5 \cdot 10^{-4}$.

The replacement of the *signum* function with the approximation $s(x)$ causes the cycle of the identified equivalent BW oscillator to enlarge (Fig. 15), thus missing the match with the reference response (Fig. 6); on the other hand, it was seen that the reintroduction of the condition upon the unloading stiffness caused the cycle of the BW system to match the reference response again (Fig. 16). A global check of the dynamic response of the modified deterministic BW model was made analyzing the dynamic response of this updated version of BW system to the El Centro NS 1940 earthquake. The comparison with the FE results, shown in Fig. 17, is satisfactory.

The proposed approximation for the *signum* function allows Eqs. (22) and (23) to be written as follows:

$$\begin{aligned} &m\ddot{\bar{x}}(t) + c\dot{\bar{x}}(t) + kg(\bar{x},\bar{z}) = f(t) \\ &g(x_1,x_2) = \alpha x_1 + (1-\alpha)x_2 \\ &\dot{\bar{z}}(t) = \dot{\bar{x}}(t)[1 - h(\dot{\bar{x}},\bar{z})] \\ &\text{where: } h(x_1,x_2) = |x_2|^n \cdot [\beta + \gamma s(x_1)s(x_2)] \end{aligned} \tag{25}$$

and

$$\begin{aligned} &m\ddot{\bar{x}}_k(t) + c\dot{\bar{x}}_k(t) + kg(\bar{x}_k,\bar{z}_k) = -g(\bar{x},\bar{z}) \\ &\dot{\bar{z}}_k(t) = \dot{\bar{x}}_k(t)[1 - h(\dot{\bar{x}},\bar{z})] - \dot{\bar{x}}(t)[h_{,1}(\dot{\bar{x}},\bar{z})\dot{\bar{x}}_k + h_{,2}(\dot{\bar{x}},\bar{z})\bar{z}_k] \end{aligned} \tag{26}$$

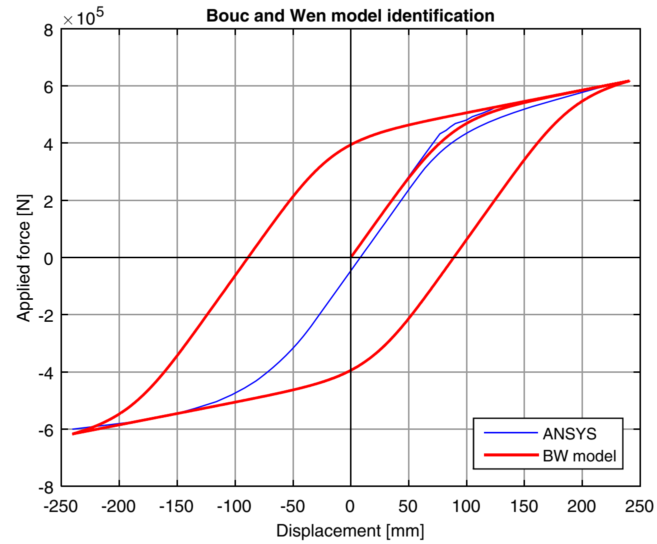

Fig. 15. Comparison of the identified BW model with the *ANSYS* results (*signum* function approximated with *s*)

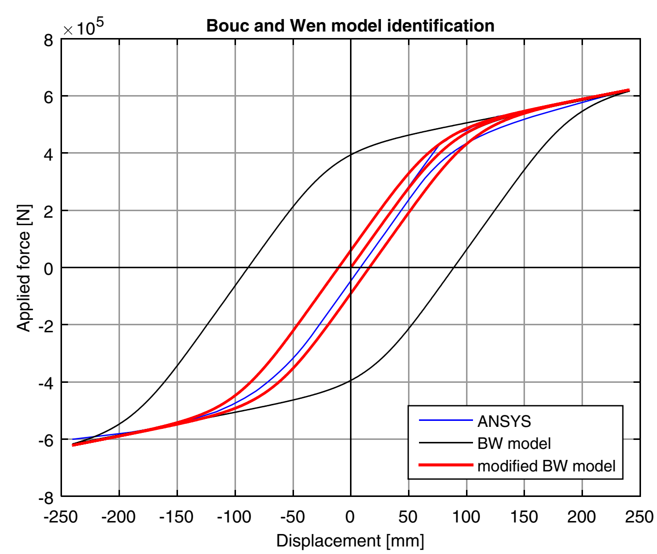

Fig. 16. Comparison of the identified BW model with the *ANSYS* results

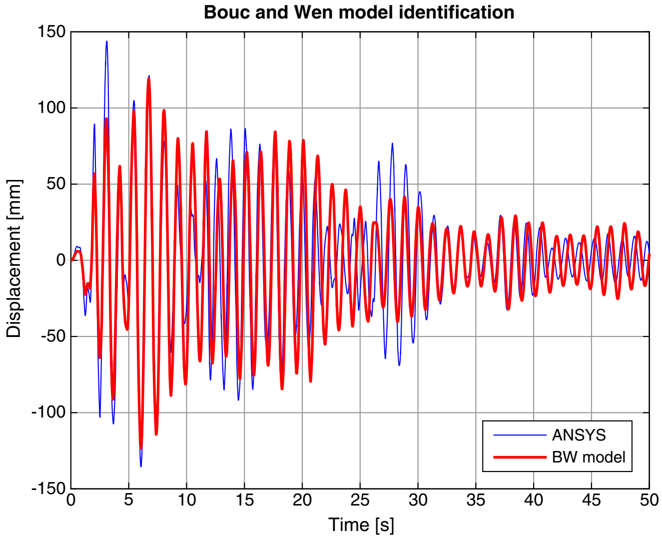

Fig. 17. Displacement time history: comparison between BW identified model and *ANSYS* results (El Centro NS 1940 earthquake)

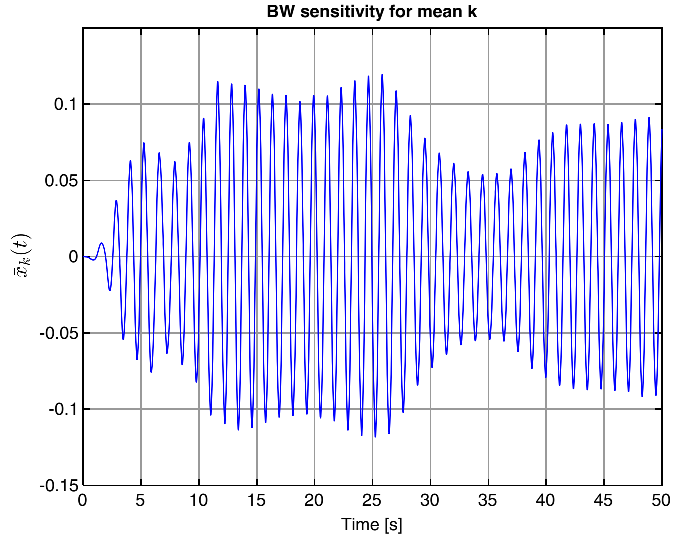

Fig. 19. Sensitivity of the response $\bar{x}_k(t)$

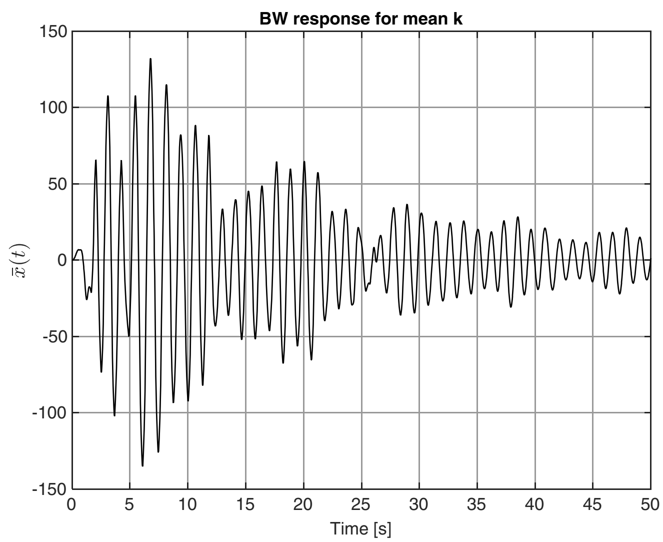

Fig. 18. Response $\bar{x}(t)$ evaluated for $\bar{k} = E[k]$

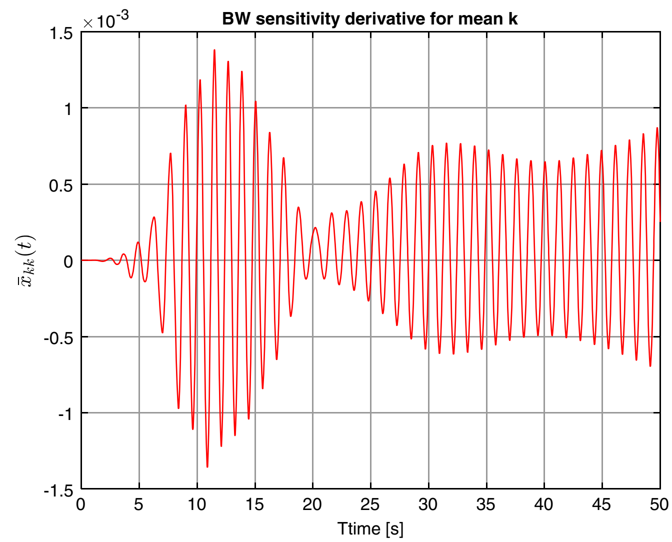

Fig. 20. Derivative of the sensitivity $\bar{x}_{kk}(t)$

A further differentiation with respect to k of the equation of motion gives the equation of motion of the second derivative of the BW response to the earthquake:

$$\begin{aligned} m\ddot{\bar{x}}_{kk}(t) + c\dot{\bar{x}}_{kk}(t) + kg(\bar{x}_{kk}, \bar{z}_{kk}) &= -2g(\bar{x}_k, \bar{z}_k) \\ \dot{\bar{z}}_{kk}(t) = \dot{\bar{x}}_{kk}(t)[1 - h(\dot{\bar{x}}, \bar{z})] - 2\dot{\bar{x}}_k(t)[h_{,1}(\dot{\bar{x}}, \bar{z})\dot{\bar{x}}_k + h_{,2}(\dot{\bar{x}}, \bar{z})\bar{z}_k] \\ - \dot{\bar{x}}(t)[h_{,11}(\dot{\bar{x}}, \bar{z})\dot{\bar{x}}_k^2 + 2h_{,12}(\dot{\bar{x}}, \bar{z})\dot{\bar{x}}_k\bar{z}_k + h_{,22}(\dot{\bar{x}}, \bar{z})\bar{z}_k^2 \\ + h_{,1}(\dot{\bar{x}}, \bar{z})\dot{\bar{x}}_{kk} + h_{,2}(\dot{\bar{x}}, \bar{z})\bar{z}_{kk}] \end{aligned} \tag{27}$$

In Eqs. (26) and (27), the notations $h_{,1}$ and $h_{,2}$ = the partial derivatives of function h with respect to x_1 and x_2, respectively. By means of the integration of Eqs. (25)–(27), which constitute a set of coupled deterministic nonlinear equations, it was possible to evaluate the sensitivity vectors and to estimate (1) the response $\bar{x}(t)$ evaluated for $\bar{k} = E[k]$ (Fig. 18); (2) the sensitivity of the response $\bar{x}_k(t)$ (Fig. 19), and (3) the derivative of the sensitivity $\bar{x}_{kk}(t)$ (Fig. 20).

The approximations for the expected value of the response, and its standard deviation, were obtained by means of a second-order expansion for the mean displacement and a first-order expansion for the variance, by

$$E[x(t)] \simeq \bar{x}(t) + 1/2\bar{x}_{kk}(t)\sigma_k^2 \qquad \sigma_x(t) \simeq \bar{x}_k(t)\sigma_k \tag{28}$$

The evaluated expected response, together with the 3σ bounds, is shown in Fig. 21.

This approach works well with a single accelerogram but, compared with the stochastic equivalent linearization, it cannot be applied in its present form with a seismic stochastic process. Further improvements will take into account the response of the disordered system to a stochastic process, instead of only one accelerogram, together with the dependence of the response on the randomness of other parameters, such as the yielding point.

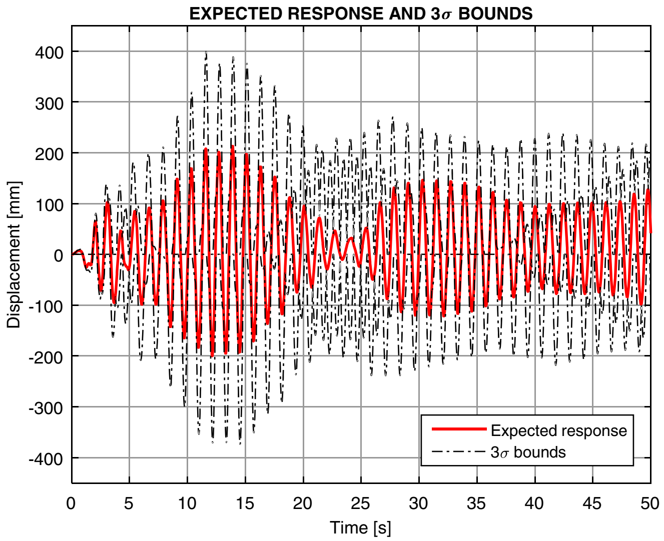

Fig. 21. Expected response and bounds of the disordered BW system

Concluding Remarks

The paper reports on a simplified and expeditious approach for the seismic analysis of disordered masonry towers and, as a clarifying example, a masonry cantilever beam was analyzed. The method, based on the assumption that the dynamic response of such class of structures is mainly ruled by its first mode shape, takes into account the randomness of the tower parameters and proposes a SDOF Bouc and Wen hysteretic model to reproduce the structural response. The parameters of the equivalent BW model were identified on the basis of nonlinear static and time-history simulations, and the paper demonstrates that the tower seismic response can be efficiently approximated by the SDOF Bouc and Wen system, provided that a proper identification of the parameters is performed. The results of the simplified approach were compared with the results of FE model to show the effectiveness of the method. The influence of a random initial stiffness of the Bouc and Wen model on its seismic response was subsequently analyzed by means of stochastic linearization and the perturbation approach to evaluate the expected response and its bounds. The perturbative approach works well with a single accelerogram, but it could not be applied with a seismic stochastic process. On the contrary an attracting feature of the equivalent linearization is that the linear response spectrum of a given site can be combined with the equivalent linear system parameters in order to obtain a inelastic response spectrum. Further improvements of the research will take into account the response of the disordered system to a stochastic process analyzing the dependence of the response on the randomness of additional parameters such as the yielding point. In addition, a thorough sensitivity analysis of the whole set of parameters of the Bouc and Wen model shall be carried out considering towers with varying slenderness in order to develop a robust model that can be employed without having pretuned parameters.

Acknowledgments

The authors kindly acknowledge the Region of Tuscany that financially supported the research (theme PAR FAS 2007-2013—CIPE n°166/2007—line 1.1.a.3: Science and Technology for the preservation and enhancement of cultural heritage).

References

Adam, J. M., Ivorra, S., Pallarés, F. J., Giménez, E., and Calderón, P. A. (2009). "Axially loaded RC columns strengthened by steel caging. Finite element modelling." *Construct. Build. Mater.*, 23(6), 2265–2276.

ANSYS 5.0 [Computer software]. Swanson Analysis Systems, Canonsburg, PA.

Bartoli, G., et al. (2013). "Confronto tra modellazioni numeriche non lineari della risposta sismica di torri in muratura." *Proc., Conf. on AID Monuments*, Aracne Editrice, Rome.

Betti, M., Bartoli, G., Corazzi, R., and Kovačević, V. (2012). "Strumenti Open Source per l'ingegneria strutturale. Modellazione meccanica non lineare di edifici in muratura." *Bollettino degli Ingegneri*, LX (12), 3–15 (in Italian).

Betti, M., Biagini, P., and Facchini, L. (2005). "Comparison among different techniques for reliability assessment of no-tensile structures under turbulent wind." *Proc., 4th European–African Conf. on Wind Engineering*, Prague, Czech Republic.

Betti, M., Galano, L., and Vignoli, A. (2014). "Comparative analysis on the seismic behaviour of unreinforced masonry buildings with flexible diaphragms." *Eng. Struct.*, 61(2014), 195–208.

Betti, M., and Vignoli, A. (2008). "Modelling and analysis of a Romanesque church under earthquake loading: Assessment of seismic resistance." *Eng. Struct.*, 30(2), 352–367.

Bouc, R. (1967). "Forced vibration of mechanical systems with hysteresis." *Proc., 4th Conf. on Nonlinear Oscillations*, Academia, Innova Park, Enfield, U.K.

Bursi, O. S., Ceravolo, R., Erlicher, S., and Zanotti Fragonara, L. (2012). "Identification of the hysteretic behaviour of a partial-strength steel-concrete moment-resisting frame structure subject to pseudodynamic tests." *Earthquake Eng. Struct. Dyn.*, 41(14), 1883–1903.

Casolo, S. (1998). "A three-dimensional model for vulnerability analysis of slender medieval masonry towers." *J. Earthquake Eng.*, 2(4), 487–512.

Chiostrini, S., and Facchini, L. (1999). "Response analysis under stochastic loading in presence of structural uncertainties." *Int. J. Numer. Meth. Eng.*, 46(6), 853–870.

Chiostrini, S., Galano, L., and Vignoli, A. (1998). "In-situ tests and numerical simulations on structural behaviour of ancient masonry." *Proc., Workshop on Seismic Performance of Monuments*, DGEMN-LNEC-JRC, Lisbon, Portugal.

Code_Aster 10.0 [Computer software]. EDF R&D–Electricity of France, Clamart, France.

Crandall, S. H., and Mark, W. D. (1963). *Random vibration in mechanical systems*, Academic Press, New York.

Cunha, A. M. F. (1994). "The role of the stochastic equivalent linearization method in the analysis of the non-linear seismic response of building structures." *Earthquake Eng. Struct. Dyn.*, 23(8), 837–857.

Decanini, L. D., Liberatore, D., Liberatore, L., and Sorrentino, L. (2012). "Preliminary report on the 2012, May 20th Emilia earthquake." ⟨http://www.eqclearinghouse.org/2012-05-20-italy-it/⟩ (May 21, 2015).

Drucker, D. C., and Prager, W. (1952). "Soil mechanics and plastic analysis or limit design." *Q. Appl. Math.*, 10(2), 157–165.

EDF R&D (Électricité de France Research and Development). (2011). "Loi de comportement ENDO_ORTH_BETON." ⟨http://www.code-aster.org/V2/doc/v11/fr/man_r/r7/r7.01.09.pdf⟩ (Feb. 3, 2012) (in French).

EDF R&D (Électricité de France Research and Development). (2012). "Modèle d'endommagement de Mazars." ⟨http://www.code-aster.org/V2/doc/v11/fr/man_r/r7/r7.01.08.pdf⟩ (May 9, 2012) (in French).

Erlicher, S., and Bursi, O.S (2008). "Bouc-Wen-type models with stiffness degradation: Thermodynamic analysis and applications." *J. Eng. Mech.*, 10.1061/(ASCE)0733-9399(2008)134:10(843), 843–855.

Facchini, L., Betti, M., and Biagini, P. (2012). "Seismic analysis of masonry towers." *Meccanica dei Materiali e delle Strutture*, 1(3), 9–20.

Facchini, L., Betti, M., Biagini, P., and Vignoli, A. (2005). "RBF– Galerkin approach for the dynamics of simple disordered masonry structures." *Atti del XVII Congresso Nazionale AIMETA di Meccanica Teorica ed Applicata, AIMETA 2005*, Firenze University Press, Firenze, Italy.

Faravelli, L., Casciati, F., and Singh, M. P. (1988). "Stochastic equivalent linearization algorithms and their applicability to hysteretic systems." *Meccanica*, 23(2), 107–112.

Foliente, G. C. (1995). "Hysteresis modelling of wood joints and structural systems." *J. Struct. Eng.*, 10.1061/(ASCE)0733-9445(1995)121:6(1013), 1013–1022.

Giaralis, A., and Spanos, P. D. (2013). "Derivation of equivalent linear properties of Bouc-Wen hysteretic systems for seismic response spectrum analysis via statistical linearization." *Proc., 10th Int. Congress on Mechanics, HSTAM 2013*, Technical Univ. of Crete, Chania, Greece.

Godard, V. (2005). "Modélisation de l'endommagement anisotrope du béton avec prise en compte de l'effet unilatéral: Application à la simulation numérique des enceintes de confinement." Thèse de doctorat d'état de l'Université Pierre et Marie Curie (Paris VI), Paris.

Ikhouane, F., Hurtado, J. E., and Rodellar, J. (2007). "Variation of the hysteresis loop with the Bouc-Wen model parameters." *Nonlinear Dyn.*, 48(4), 361–380.

Ismail, M., Ikhouane, F., and Rodellar, J. (2009). "The hysteresis Bouc-Wen model, a survey." *Arch. Comput. Meth. Eng.*, 16(2), 161–188.

Ismail, M., Rodellar, J., and Ikhouane, F. (2010). "An innovative isolation device for aseismic design." *Eng. Struct.*, 32(4), 1168–1183.

Liu, W. K., Belytschko, T., and Mani, A. (1986). "Probabilistic finite elements for non-linear structural dynamics." *Comput. Meth. Appl. Mech. Eng.*, 56(1), 61–81.

Lucchesi, M., and Pintucchi, B. (2007). "A numerical model for non-linear dynamics analysis of masonry slender structures." *Eur. J. Mech. A/Solids*, 26(1), 88–105.

Marano, G. C., and Greco, R. (2006). "Damage and ductility demand spectra assessment of hysteretic degrading systems subject to stochastic seismic loads." *J. Earthquake Eng.*, 10(5), 615–640.

Mazars, J. (1984). "Application de la mécanique de l'endommagement au comportement non linéaire et à la rupture du béton de structure." Thèse de doctorat d'état de l'Université Pierre et Marie Curie (Paris VI), Laboratoire de mécanique et technologie, Paris.

Milani, G., and Valente, M. (2015). "Failure analysis of seven masonry churches severely damaged during the 2012 Emilia-Romagna (Italy) earthquake: Non-linear dynamic analyses vs conventional static approaches." *Eng. Fail. Anal.*, 54(2015), 13–56.

Oldfield, M., Ouyang, H., and Mottershead, J. E. (2005). "Simplified models of bolted joints under harmonic loading." *Comput. Struct.*, 84(1–2), 25–33.

Ortiz, G. A., Alvarez, D. A., and Bedoya-Ruíz, D. (2013). "Identification of Bouc–Wen type models using multi-objective optimization algorithms." *Comput. Struct.*, 114–115(2013), 121–132.

Roberts, J. B., and Spanos, P. D. (2003). *Random vibration and statistical linearization*, Dover, NY.

Wang, C. H., and Chang, S. Y. (2007). "Development and validation of a generalized biaxial hysteresis model." *J. Eng. Mech.*, 10.1061/(ASCE)0733-9399(2007)133:2(141), 141–152.

Wen, Y. K. (1976). "Method for random vibration of hysteretic systems." *J. Eng. Mech. Div.*, 103(2), 249–263.

Wen, Y. K. (1980). "Equivalent linearization for hysteretic systems under random excitation." *J. Appl. Mech.*, 47(1), 150–154.

Willam, K. J., and Warnke, E. D. (1975). "Constitutive model for the triaxial behaviour of concrete." *Proc., Int. Association for Bridge and Structural Engineering*, IABSE, Zurich, Switzerland.